Check for updates

Chiral recognition *via* a stereodynamic vanadium probe using the electronic circular dichroism effect in differential Raman scattering†

Ewa Machalska,‡[ab] Natalia Hachlica,‡[ab] Grzegorz Zajac, [iD][bc] Davide Carraro,[d] Malgorzata Baranska, [iD][ab] Giulia Licini,[d] Petr Bouř, [iD]*[c] Cristiano Zonta [iD]*[d] and Agnieszka Kaczor [iD]*[ab]

Intermolecular interactions sensitive to chirality occur in many biological events. We report a complex formation between a versatile vanadium-based probe and a chiral co-ligand monitored *via* the combination of electronic circular dichroism (ECD) and Raman scattering. This ''ECD-Raman'' effect was discovered relatively recently and can be measured using a Raman optical activity (ROA) spectrometer. Simulated spectra based on experimental ECD and degree of circularity (DOC) values agree with the observed ones. Sensitive recognition of the chiral enantiopure co-ligand is thus enabled by a combination of resonance of the excitation light with the diastereoisomeric complex, co-ligand complexation, circular dichroism, and polarized Raman scattering from the achiral solvent. Relatively dilute solutions could be detected (10^{-4} mol dm^{-3}), about 1000× less than is necessary for conventional ROA detection of the pure co-ligand and comparable to concentrations needed for conventional ECD spectroscopy. The results thus show that differential ECD-Raman measurements can be conveniently used to monitor molecular interactions and molecular spectroscopic properties.

Introduction

Chiroptical chemistry has proved to be useful for a wide range of technological and biomedical applications. A prominent example is the Nobel-prize winning idea of chiroptical switching that finally evolved into molecular motors.[1] Other challenges and perspectives associated with chiroptical molecular switches comprise control of motion, trigger driven LD devices and control of surfaces and interfaces.[1,2] Chiral recognition enables direct sensing of a chiral analyte by a sensor and can be used for determination of the enantiomeric excess (EE) and absolute configuration (AC). Chiral methods were proposed for in-line and point-of-care analysis and design of drugs.[3]

Stereodynamic probes are often built from rapidly interconverting stereoisomers, where one form is stabilized by interactions with a chiral analyte, yielding an enhanced chiroptical signal.[4,5] Efficient stereodynamic sensor needs to combine this chiral recognition with a strong measurable response, such as electronic circular dichroism (ECD), vibrational circular dichroism (VCD)[6] and circular polarized luminescence (CPL).[7]

Also Raman optical activity (ROA) was utilized as a versatile method for the detection of chiral compounds. This technique registers a tiny difference in Raman scattering intensities of right- and left-handed circularly polarized light ($I_R - I_L$). However, ROA usually requires rather high analyte concentrations and long measurement times. Various attempts to enhance the signal appeared in the past.[8–13] For example, metal nanoparticles might induce a chiral response in an achiral reporter molecule.[14]

In the present study, we explore another effect, first studied on a metal complex inducing a $I_R - I_L$ response in achiral solvents.[15] This was originally attributed to a ''ring of fire'', a solvent region 8–10 Å away from the metal.[15] However, more recent works based on carefully designed experiments and calculations unambiguously demonstrated that the observed signal is due to a combination of ECD and polarized Raman scattering (ECD-Raman).[16–18] In the most common scattered circular polarization (SCP) experiment the chiral component in

a Faculty of Chemistry, Jagiellonian University, Gronostajowa 2, Krakow 30-387, Poland. E-mail: agnieszka.kaczor@uj.edu.pl

b Jagiellonian Centre for Experimental Therapeutics (JCET), Jagiellonian University, Bobrzynskiego 14, Krakow 30-348, Poland

c Institute of Organic Chemistry and Biochemistry, Academy of Sciences, Flemingovo náměstí 2, 16610, Prague, Czech Republic. E-mail: petr.bour@uochb.cas.cz

d Dipartimento di Scienze Chimiche, Università degli Studi di Padova and CIRCC, Padova Unit, 35131 Padova, Italy. E-mail: cristiano.zonta@unipd.it

† Electronic supplementary information (ESI) available: Description of materials and methods, detailed description of quantum-chemical calculations, and additional spectra helpful in the analysis of the results. See DOI: 10.1039/d1cp03020e

‡ These authors contributed equally.

23336 | *Phys. Chem. Chem. Phys.*, 2021, **23**, 23336–23340

This journal is © the Owner Societies 2021

the sample polarizes the light through ECD, and the light polarization is further changed in the course of Raman scattering. The proposed theory correctly predicted signs and intensities of solvent bands observed in ROA spectra.[16] However, extensive analytical applications of this methodology have not been explored yet.

A chiral ligand is used with a vanadium-based complex as the model chiroptical sensor. The results show that the recognition of the chiral analyte leads to an intense ECD-Raman differential effect that can be detected by the ROA spectrometer as a strong signal of the solvent. The band signs are dictated by the chirality of the ligand and solvent's degrees of circularity (DOC), as predicted by recent works dedicated to the ECD-Raman effect and natural resonance ROA.[16,17]

Results and discussion

Ligand-dependent ECD-Raman signal of achiral solvents

The studied chiral probe, oxo-vanadium(v) aminotriphenolate, was originally proposed as a CD stereodynamic sensor for a large variety of chiral analytes.[19] In the absence of a chiral co-ligand, the vanadium complex makes an ECD-silent racemic mixture of interconverting stereoisomers (ESI,† Fig. S1). In the presence of the chiral analyte, for example (R) or (S)-N-(1-phenylethyl)acetamide, two diastereoisomers are formed in different proportions[19] giving an intense ECD signal in the visible range (Fig. 1).

The third component of the system, the solvent, does not participate in electronic absorption or ECD. Similarly, natural ROA of the supramolecular unit is not detectable and its Raman

Fig. 1 ECD, Raman and ROA (mostly ECD-Raman) spectra of systems composed of oxo-vanadium(v) aminotriphenolate and S and R enantiomers of N-(1-phenylethyl)acetamide in various concentrations in CHCl₃.

bands are weak. However, the enantiomeric enrichment of the chiral system is detected in ROA measurements as the ECD-Raman solvent bands. This is shown in Fig. 1. Strong Raman bands are visible at 260, 367, 671, 760 and 1218 cm⁻¹, and less intense signals are present at 488, 509, 564, 1113, 1276, 1300, 1367, 1424, 1446, 1461 and 1584 cm⁻¹, the positions of which slightly depend on the co-ligand and complex concentrations (ESI,† Fig. S2). Most of them could be assigned to the vanadium(v) complex itself. In particular, bands at 500, 527, 1262 and 1283 cm⁻¹ of the pure complex change position as a result of the substrate binding. Solvent bands occur at 260, 367, 671, 760 and 1220 cm⁻¹ and they also produce the ECD-Raman bands observed in the ROA measurements (Fig. 1, right). This was verified with a racemic mixture of the co-ligand (ESI,† Fig. S3). ECD-Raman spectra of R and S enantiomers of N-(1-phenylethyl)acetamide are near "mirror images". The "mirror-image" symmetry is not observed for the bands at 367 and 671 cm⁻¹; this can be, however, explained by polarization artefacts for these strongly polarized bands.[20] For the other bands, the signs for a given stereoisomer agree with the sign of ECD within 532–572 nm.

ECD-Raman spectra modelling

Although the ECD-Raman effect is relatively complex (ECD of excitation light, re-polarization during the Raman scattering, ECD of the scattered light, potential mix of the differential signal with natural/true ROA), it is now relatively well understood and can be reliably identified and simulated.[16–18] For our data, the DOC values[20] required to simulate the ECD-Raman intensities were determined from the experiment (ESI,† Fig. S4, using the DOC option in the spectrometer software). Corresponding CID values were determined from:[16]

$$ CID = \frac{I_R - I_L}{I_R + I_L} = \frac{\Delta\varepsilon' + DOC \cdot \Delta\varepsilon}{4} \ln 10 cL \qquad (1) $$

where I_R and I_L are Raman intensities of right- and left-circularly polarized scattered light, respectively. $\Delta\varepsilon$ and $\Delta\varepsilon'$ (L mol⁻¹ cm⁻¹) are differential molar extinction coefficients for the incident and scattered light, respectively, c (mol L⁻¹) is concentration, and L (cm) is the optical pathlength. In terms of ellipticities,

$$ CID = \frac{I_R - I_L}{I_R + I_L} = \frac{\theta_s' + DOC\,\theta_s}{131\,952} \ln 10 \frac{L}{l} \qquad (2) $$

where θ_s and θ_s' (mdeg) are ellipticity values for the incident and scattered light, respectively, and l (cm) is the pathlength in the ECD experiment. This formula provided an excellent basis for interpretation of our results, although the CIDs were somewhat smaller than the experimental ones because of the laser focusing (Fig. 2A and ESI,† Table S1). Indeed, formula (1) was derived for uniform scattering and ECD along the laser beam, whereas the real scattering is limited to a smaller volume (Fig. 2B).

A comparison of simulated ECD-Raman and experimental spectra is given in Fig. 3. Except for the uncertainty given by the non-ideal experimental setup, the calculated spectra faithfully reproduce the experiment. The ECD-Raman theory[16] thus
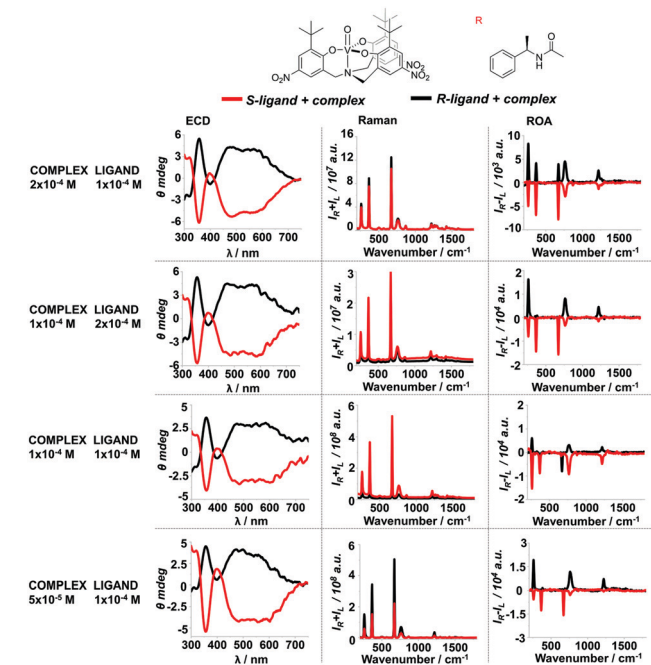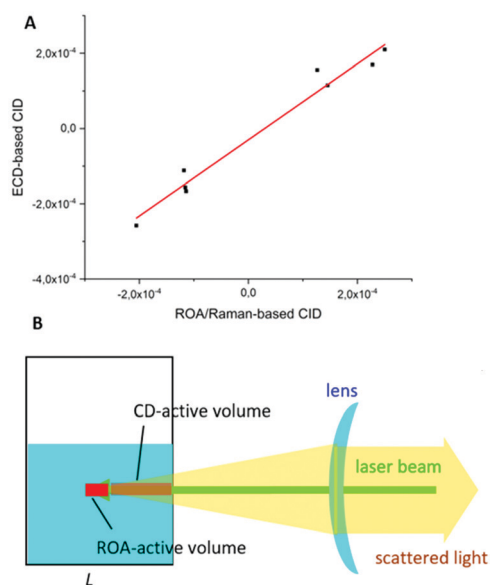
This journal is © the Owner Societies 2021

Phys. Chem. Chem. Phys., 2021, **23**, 23336–23340 | **23337**

Fig. 2 Correlation between calculated and experimental CID values, for the band at 760 cm^{-1} (r-square = 0.972) (A) and schematic showing laser focusing in the ROA experiment (B).
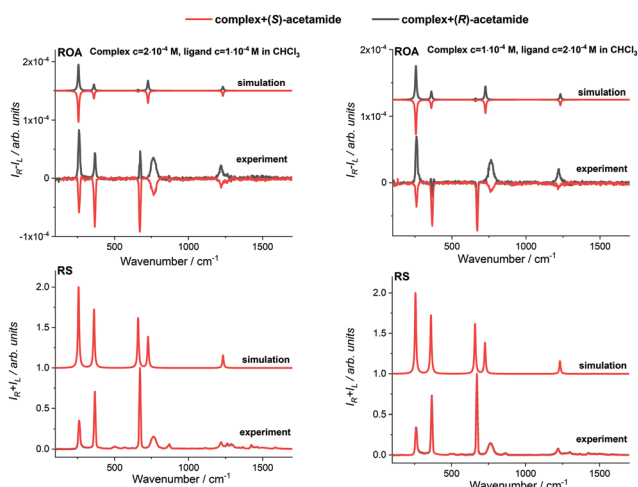

Fig. 3 Comparison of experimental Raman and ROA (mostly ECD-Raman) spectra with simulated Raman and ECD-Raman spectra in the system composed of oxo-vanadium(v) aminotriphenolate and S and R enantiomers of N-(1-phenylethyl)acetamide in CHCl$_3$. The spectra were normalized while preserving the CID ratios.

enables accurate predictions of the intensities and signs of solvent bands also for the system composed of the stereodynamic probe and a chiral co-ligand. R and S enantiomers of N-(1-phenylethyl)acetamide give positive and negative spectra, respectively. Although formulas permit different signs for different bands, in our case the sign does not change because of $\Delta\varepsilon' > $ DOC·$\Delta\varepsilon$ for the R stereoisomer and $\Delta\varepsilon' < $ DOC·$\Delta\varepsilon$ for the S stereoisomer, for all studied Raman solvent bands.

The ECD-Raman signal can be measured for very low concentrations of the co-ligand, smaller than 10^{-4} mol dm^{-3}. This

corresponds to about 2 micrograms of the compound and is similar to the usual needs of conventional ECD spectroscopy, while milligram amounts are necessary to obtain a good ROA spectrum of the pure enantiopure co-ligand (ESI,† Fig. S5). Note that at the applied concentrations no vibrational ROA of the complex or ligand can be observed.

To summarize these results, the chiral, enantiopure co-ligand makes a preferential diastereoisomeric assembly with the stereodynamic vanadium complex, the electronic states of which are in resonance with the laser beam and cause circular dichroism, which leads to the ECD-Raman response of the achiral solvent. ECD of the probes based on oxo-vanadium(v) aminotriphenolate was found to be independent of the concentration of the complex and the g-factors were linearly dependent on EE of the co-ligand.[19] CID values based on the ECD/DOC values are about linearly dependent on the concentration of the co-ligand for constant complex concentration and *vice versa* (ESI,† Fig. S6).

Variation of the solvents

The system was measured also in CH$_2$Cl$_2$ and CH$_3$CN (Fig. 4). Similar behaviour suggests that the structure of the complex is similar and that the ECD-Raman detection is universal for all solvents. The spectra are nearly mirror images for the two enantiomers of N-(1-phenylethyl)acetamide, except for a few polarized bands (at 705 cm^{-1} for CH$_2$Cl$_2$; 920 and 2260 cm^{-1} for CH$_3$CN). Signals of CH$_2$Cl$_2$ appear at 284, 706, 744, 1160 and 1427 cm^{-1}. For CH$_3$CN, bands are observed at 380, 920, 1377, 1446 and 2261 cm^{-1}.

Raman bands of the co-ligand/complex unit formed in CH$_3$CN are more visible than for CHCl$_3$ and CH$_2$Cl$_2$, which can be attributed to a change of the resonance conditions and a weaker ECD intensity at 532 nm. Some vibrational ROA of the
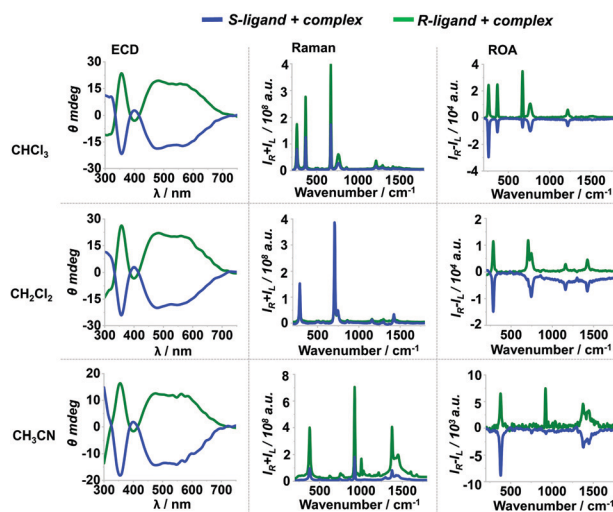

Fig. 4 ECD, Raman and ROA (mostly ECD-Raman) spectra of the supramolecule composed of oxo-vanadium(v) aminotriphenolate and S and R enantiomers of N-(1-phenylethyl)acetamide in CHCl$_3$, CH$_2$Cl$_2$, and CH$_3$CN. The ligand and complex concentrations are 8×10^{-4} mol dm^{-3} and 1×10^{-4} mol dm^{-3}, respectively.
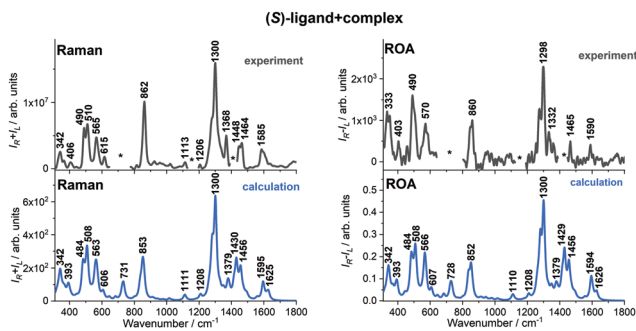
Fig. 5 Comparison of experimental and DFT calculated Raman and ROA spectra of the supramolecule composed of oxo-vanadium(v) aminotri-phenolate and (S)-N-(1-phenylethyl)acetamide in CH₂Cl₂. The ligand and complex concentrations are 8×10^{-4} M and 1×10^{-4} M, respectively (1 : 8 ratio). Calculated frequencies were multiplied by a factor of 0.9745 to fit to the experimental ones. Asterisks denote ranges, where Raman or ECD-Raman bands of the solvent were subtracted (for clarity).

complex could be detected in CH₂Cl₂ at detector oversaturation conditions (ESI,† Fig. S7, detector is saturated by the solvent bands), using higher laser powers and chiral co-ligand concentrations.

Resonance ROA of the complex–ligand system

DFT calculations of the ROA and Raman spectra of the complex–(S)–ligand system confirm that the registered weak signals, although very noisy, are RROA of the solute (Fig. 5 and ESI,† Fig S8). As predicted by the single electronic state theory the spectra are monosignate and their sign is opposite to the ECD of the electronic transition in resonance with the laser beam. Despite the good agreement with the RROA theory, it is worth stressing that the recorded RROA can also be affected by the ECD-Raman of the solute itself. As shown recently, depending on the measuring conditions, measured compound, and its spectroscopic properties, either the RROA or ECD-Raman signal may dominate.[18] Here, because the RROA sign is opposite to the ECD, one can say that the RROA dominates. It clearly shows that for the studied system, recording RROA of the solute requires markedly increased laser power (as shown) or higher ligand/complex concentrations compared to the ECD-Raman signal of the solvents.

Conclusions

With a growing number of new pharmaceuticals, there is a need for straightforward and reliable methods for determination of their EE. Non-resonant ROA requires high concentrations of analytes and long measurement times. Therefore, these methods can be complemented by the somewhat complex, but universal ECD-Raman effect. In our case it provided chiral recognition of enantioenriched analytes as co-ligands. ECD-Raman spectra can be recorded in a relatively short time for reasonably low concentrations of the analyte. For N-(1-phenylethyl)acetamide, clear spectra were obtained using only 2 micrograms of the compound, hence the sensitivity of the

method is comparable to the conventional ECD spectroscopy. The vanadium ECD-Raman stereodynamic probe may be applied for a wide range of chiral small molecules containing different chemical functions.

Materials and methods

Preparation of the complex–ligand system

R and S enantiomers of N-(1-phenylethyl)acetamide (the chiral ligand) as well as oxo-vanadium(v) aminotriphenolate (referred to in the following text as the complex) were synthesized via a previously reported procedure.[19] All solvents (i.e. CHCl₃, CH₂Cl₂ and CH₃CN) were purchased from Sigma Aldrich and used as received. Stock solutions of the complex (2×10^{-3} mol dm⁻³) and the chiral ligand (8×10^{-3} mol dm⁻³) were prepared in three different anhydrous solvents in different ratios for CHCl₃. The sample was prepared by mixing determined amounts of the ligand and solvent solutions and subsequently diluting to reach 1 or 5 mL volume (depending on the ECD cuvette used).

Spectra measurements

All solutions were passed through the Millex® syringe PTFE filters (of a pore size of 0.45 μm) to remove solid impurities before recording Raman and ROA spectra. Raman and ECD-Raman/ROA spectra were measured using a ChiralRAMAN-2X™ spectrometer (BioTools Inc.) at a resolution of 7 cm⁻¹ with the excitation wavelength of 532 nm with integration time of 2 s and 19–24 hour acquisition time. The laser power (80–200 mW) has been adjusted is such a way that the detector saturation remained approximately the same for every ROA/Raman measurement. For some experiments an oversaturation and higher laser powers were used (300–850 mW, ESI,† Fig. S7). The concentrations were 8×10^{-4} mol dm⁻³ and 1×10^{-4} mol dm⁻³ for the ligand and complex, respectively, and at least two different Raman/ROA experiments were conducted (ESI,† Fig. S9).

DOC spectra were measured using the same ChiralRAMAN-2X™ spectrometer with the integration time of 2 s for 30 s with the laser power of 10–20 mW. Raman and ROA spectra for the background signal were corrected using the OriginPro or OPUS software. The ROA spectra obtained were smoothed using the Savitzky–Golay procedure with OriginPro.

UV-Vis and ECD spectra of solutions containing the complex and chiral ligand were recorded in the 300–750 nm spectral range using quartz cells with a path length of 10 mm (samples with the ligand concentration of 8×10^{-4} mol dm⁻³) or 2 mm (all others), a scanning speed of 100 nm min⁻¹, a bandwidth of 1 nm, 0.5 s response time and accumulation of 1 or 5 scans on a Jasco J-815 spectrometer. The concentrations of all components were the same as for Raman/ROA measurements (the same samples were measured). Minor background correction and smoothing of the registered spectra were done using JASCO and OriginPro software.

Computational details

ECD-Raman spectra of the solvent (CHCl₃) in the oxo-vanadium(v) aminotriphenolate and (S)-N-(1-phenylethyl)acetamide systems

This journal is © the Owner Societies 2021

Phys. Chem. Chem. Phys., 2021, **23**, 23336–23340 | **23339**

(Fig. 3) were calculated according to formula 1, and procedures described in ref. 16. To calculate ECD-Raman spectra of the solvent, experimental $\Delta\varepsilon'$ and $\Delta\varepsilon$ of the solute were used, along with the experimental DOC factors of the $CHCl_3$, using 0.2 cm path length and experimental solute/ligand concentrations. Geometry optimization, frequencies and Raman intensities (532 nm excitation) of the solvent were calculated using the Gaussian G16.C01 program[21] and the B3LYP/6-311++G(2d,2p) theory level.

Geometries of oxo-vanadium(v) aminotriphenolate and (S)-N-(1-phenylethyl)acetamide (CCDC 1568016)[16] were optimized using the B3LYP/6-31G(d) theory level for H, C, O and N atoms, and the MDF10 pseudopotential and basis set for the V atom, using Gaussian G16.C01 software.[21] Electronic transition energies, UV-vis and ECD intensities, vibrational frequencies, ROA and Raman intensities were obtained at the same level. Different excitation wavelengths were input to find the best match for the experimental resonance conditions (energy gap between the laser frequency and electronic transition energy). Because theoretical UV-vis and ECD band positions were blue shifted compared to the experimental ones, the wavelength used in the calculations needed to be shifted as well. The best agreement with the experiment was found for 490 nm excitation (Fig. 5 and ESI,† Fig. S8). Convoluted spectral intensities were calculated using ECD/UV with Gaussian functions of 0.1 eV half width at half maximum. For Raman/ROA Lorentzian functions and 10 cm^{-1} were used.

Author contributions

Conceptualization A. K., C. Z., P. B., funding acquisition A. K., P. B., investigation N. H., E. M., G. Z., A. K., P. B., C. Z., D. C., methodology N. C., G. Z., E. M., A. K., P. B., C. Z., G. L. software P. B., supervision A. K., visualization N. C., G. Z., E. M., A. K., P. B., writing – original draft A. K., N. H., G. Z., writing – review & editing A. K., G. Z., N. C., P. B., C. Z., E. M., G. L., D. C., M. B.

Conflicts of interest

There are no conflicts to declare.

Acknowledgements

References

1 B. L. Feringa, *Angew. Chem., Int. Ed.*, 2017, **56**, 11060–11078.

2 B. L. Feringa, R. A. Van Delden, N. Koumura and E. M. Geertsema, *Chem. Rev.*, 2000, **100**, 1789–1816.

3 J. R. Brandt, F. Salerno and M. J. Fuchter, *Nat. Rev. Chem.*, 2017, **1**, 0045.

4 B. T. Herrera, S. L. Pilicer, E. V. Anslyn, L. A. Joyce and C. Wolf, *J. Am. Chem. Soc.*, 2018, **140**, 10385–10401.

5 S. L. Pilicer, J. M. Dragna, A. Garland, C. J. Welch, E. V. Anslyn and C. Wolf, *J. Org. Chem.*, 2020, **85**, 10858–10864.

6 R. Berardozzi, E. Badetti, N. A. Carmo Dos Santos, K. Wurst, G. Licini, G. Pescitelli, C. Zonta and L. Di Bari, *Chem. Commun.*, 2016, **52**, 8428–8431.

7 N. A. Carmo dos Santos, E. Badetti, G. Licini, S. Abbate, G. Longhi and C. Zonta, *Chirality*, 2018, **30**, 65–73.

8 J. Bogaerts and C. Johannessen, *J. Raman Spectrosc.*, 2019, **50**, 641–646.

9 M. Dudek, E. Machalska, T. Oleszkiewicz, E. Grzebelus, R. Baranski, P. Szcześniak, J. Mlynarski, G. Zajac, A. Kaczor and M. Baranska, *Angew. Chem., Int. Ed.*, 2019, **58**, 8383–8388.

10 T. Fujisawa, R. L. Leverenz, M. Nagamine, C. A. Kerfeld and M. Unno, *J. Am. Chem. Soc.*, 2017, **139**, 10456–10460.

11 C. Merten, H. Li and L. A. Nafie, *J. Phys. Chem. A*, 2012, **116**, 7329–7336.

12 J. Šebestík, F. Teplý, I. Císařová, J. Vávra, D. Koval and P. Bouř, *Chem. Commun.*, 2016, **52**, 6257–6260.

13 G. Zajac, A. Kaczor, A. Pallares Zazo, J. Mlynarski, M. Dudek and M. Baranska, *J. Phys. Chem. B*, 2016, **120**, 4028–4033.

14 S. Ostovar Pour, L. Rocks, K. Faulds, D. Graham, V. Parchaňský, P. Bouř and E. W. Blanch, *Nat. Chem.*, 2015, **7**, 591–596.

15 G. Li, J. Kessler, J. Cheramy, T. Wu, M. R. Poopari, P. Bouř and Y. Xu, *Angew. Chem., Int. Ed.*, 2019, **58**, 16495–16498.

16 T. Wu, G. Li, J. Kapitán, J. Kessler, Y. Xu and P. Bouř, *Angew. Chem., Int. Ed.*, 2020, **59**, 21895–21898.

17 G. Li, M. Alshalalfeh, Y. Yang, J. R. Cheesman, P. Bouř and Y. Xu, *Angew. Chem., Int. Ed.*, 2021, **60**, 22004–22009.

18 E. Machalska, G. Zajac, A. J. Wierzba, J. Kapitán, T. Andruniów, M. Spiegel, D. Gryko, P. Bouř and M. Baranska, *Angew. Chem., Int. Ed.*, 2021, **60**, 21205–21210.

19 P. Zardi, K. Wurst, G. Licini and C. Zonta, *J. Am. Chem. Soc.*, 2017, **139**, 15616–15619.

20 L. D. Barron, *Molecular Light Scattering and Optical Activity*, Cambridge University Press, Cambridge, 2nd edn, 2004.

21 M. J. Frisch, G. W. Trucks, H. B. Schlegel, G. E. Scuseria, M. A. Robb, J. R. Cheeseman, G. Scalmani, V. Barone, G. A. Petersson, H. Nakatsuji, X. Li, M. Caricato, A. V. Marenich, J. Bloino, B. G. Janesko, R. Gomperts, B. Mennucci, H. P. Hratchian, J. V. Ortiz, A. F. Izmaylov, J. L. Sonnenberg, D. Williams-Young, F. Ding, F. Lipparini, F. Egidi, J. Goings, B. Peng, A. Petrone, T. Henderson, D. Ranasinghe, V. G. Zakrzewski, J. Gao, N. Rega, G. Zheng, W. Liang, M. Hada, M. Ehara, K. Toyota, R. Fukuda, J. Hasegawa, M. Ishida, T. Nakajima, Y. Honda, O. Kitao, H. Nakai, T. Vreven, K. Throssell, J. A. Montgomery Jr., J. E. Peralta, F. Ogliaro, M. J. Bearpark, J. J. Heyd, E. N. Brothers, K. N. Kudin, V. N. Staroverov, T. A. Keith, R. Kobayashi, J. Normand, K. Raghavachari, A. P. Rendell, J. C. Burant, S. S. Iyengar, J. Tomasi, M. Cossi, J. M. Millam, M. Klene, C. Adamo, R. Cammi, J. W. Ochterski, R. L. Martin, K. Morokuma, O. Farkas, J. B. Foresman and D. J. Fox, *Gaussian 16, Revision C.01*, Gaussian, Inc., Wallingford CT, 2016.